Tamoxifen Resistance in Breast Cancer Is Regulated by the EZH2–ERα–GREB1 Transcriptional Axis

Yanming Wu[1], Zhao Zhang[1], Mauro E. Cenciarini[2], Cecilia J. Proietti[2], Matias Amasino[2], Tao Hong[1,3], Mei Yang[1], Yiji Liao[1], Huai-Chin Chiang[1,4], Virginia G. Kaklamani[5], Rinath Jeselsohn[6,7], Ratna K. Vadlamudi[8], Tim Hui-Ming Huang[1,4], Rong Li[1,4], Carmine De Angelis[9], Xiaoyong Fu[9], Patricia V. Elizalde[2], Rachel Schiff[9,10], Myles Brown[6,7], and Kexin Xu[1,4]

Abstract

Resistance to cancer treatment can be driven by epigenetic reprogramming of specific transcriptomes in favor of the refractory phenotypes. Here we discover that tamoxifen resistance in breast cancer is driven by a regulatory axis consisting of a master transcription factor, its cofactor, and an epigenetic regulator. The oncogenic histone methyltransferase EZH2 conferred tamoxifen resistance by silencing the expression of the estrogen receptor α (ERα) cofactor GREB1. In clinical specimens, induction of DNA methylation of a particular CpG-enriched region at the *GREB1* promoter negatively correlated with *GREB1* levels and cell sensitivity to endocrine agents. GREB1 also ensured proper cellular reactions to different ligands by recruiting distinct sets of ERα cofactors to *cis*-regulatory elements, which explains the contradictory biological effects of GREB1 on breast cancer cell growth in response to estrogen or antiestrogen. In refractory cells, EZH2-dependent repression of GREB1 triggered chromatin reallocation of ERα coregulators, converting the antiestrogen into an agonist. In clinical specimens from patients receiving adjuvant tamoxifen treatment, expression levels of EZH2 and GREB1 were correlated negatively, and taken together better predicted patient responses to endocrine therapy. Overall, our work suggests a new strategy to overcome endocrine resistance in metastatic breast cancer by targeting a particular epigenetic program.

Significance: This study suggests a new strategy to overcome endocrine resistance in metastatic breast cancer by targeting a particular epigenetic program defined within. *Cancer Res; 78(3); 671–84. ©2017 AACR.*

Introduction

Tamoxifen, by competing with the hormone estrogen for binding to the receptor (ERα) in mammary tissues, is one of the commonly prescribed endocrine agents for both early and advanced ER-positive (ER⁺) breast cancer. Unfortunately, a serious limitation of this endocrine therapy is the development of acquired resistance. Substantial evidence suggests that changes of components along the ERα axis, such as altered expression of ERα cofactors, may reprogram ERα-mediated transcriptome that underlie the development of endocrine resistance (1). Recently, growth regulation by estrogen in breast cancer 1 (GREB1) was identified as the strongest interactor of estrogen-liganded, but not tamoxifen-liganded ERα (2). GREB1 enhances ERα-mediated gene expression and cell proliferation upon estrogen stimulation (2, 3), but blocks the growth of tamoxifen-resistant (TamR) breast cancer cells (2). Considering that GREB1 is a critical regulatory protein of ERα activity and that it exerts differential biological functions in tamoxifen-sensitive versus tamoxifen-refractory cells, GREB1–ERα axis may play a pivotal role in determining cell fate in response to the antiestrogen treatment.

As a highly evolving process, endocrine resistance originates from a number of mechanisms. One of the critical contributory factors is the epigenetic alteration occurring at individual driver genes or even to the whole transcriptional network (4, 5). Histone methyltransferase EZH2 has a well-demonstrated role in the progression of aggressive cancers (6–8). EZH2 methylates lysine 27 on histone H3 and thereby represses transcription of target genes (9). In addition, EZH2 is shown to directly interact with DNA methyltransferases and functionally govern DNA methylation, centering EZH2 at a pivotal position linking two critical epigenetic programs (10–12). Although roles of EZH2 in driving

[1]Department of Molecular Medicine, University of Texas Health Science Center, San Antonio, Texas. [2]Laboratory of Molecular Mechanisms of Carcinogenesis, Instituto de Biología y Medicina Experimental, CONICET, Buenos Aires, Argentina. [3]Xiangya School of Medicine, Central South University, Changsha, Hunan, P.R. China. [4]Cancer Therapy & Research Center, University of Texas Health Science Center, San Antonio, Texas. [5]Division of Hematology/Oncology, Breast Cancer Program, Cancer Therapy & Research Center, School of Medicine, University of Texas, San Antonio, Texas. [6]Center for Functional Cancer Epigenetics, Dana-Farber Cancer Institute, Boston, Massachusetts. [7]Department of Medical Oncology, Dana-Farber Cancer Institute and Department of Medicine, Harvard Medical School, Boston, Massachusetts. [8]Department of Obstetrics and Gynecology, Cancer Therapy & Research Center, University of Texas Health Science Center, San Antonio, Texas. [9]Department of Molecular and Cellular Biology, Lester & Sue Smith Breast Center, Dan L. Duncan Cancer Center, Baylor College of Medicine, Houston. [10]Department of Medicine, Baylor College of Medicine, Houston.

Note: Supplementary data for this article are available at Cancer Research Online (http://cancerres.aacrjournals.org/).

Z. Zhang, M.E. Cenciarini, and C.J. Proietti contributed equally to this article.

Corresponding Author: Kexin Xu, University of Texas Health Science Center at San Antonio, 8403 Floyd Curl Dr., San Antonio, TX 78229. Phone: 210-562-4148; Fax: 210-562-4161; E-mail: XuK3@uthscsa.edu

cancer progression are extensively characterized, few studies investigate the association of EZH2 with acquired drug resistance. In particular, with the small-molecule inhibitors of EZH2 available (13, 14), it is important to test whether pharmacologic inhibition of EZH2 will hold promise in the treatment of therapy-resistant cancers.

In this study, we demonstrated that EZH2-mediated epigenetic silencing of ERα cofactor GREB1, conceivably through DNA methylation, reprograms ERα-dependent transcriptional machinery, which leads to the refractory phenotype in breast cancer cells. We revealed an important transcriptional axis comprised of ERα, EZH2, and GREB1 in driving the development of tamoxifen resistance.

Materials and Methods

Plasmids and siRNAs

Human pLenti-CMV-HA-Hygro-EZH2 was generously provided by Dr. Lixin Wan (H. Lee Moffitt Cancer Center, Tampa, FL). EZH2-specific shRNAs were generated as reported previously (15). Both of shGREB1-1 and -2 (TRCN0000273201 and TRCN0000000290) were purchased from Sigma, and siGREB1 (M-008187-01-0005) was obtained from Dharmacon.

Antibodies and reagents

Antibodies being used in this study for Western blots include: anti-GREB1 (#ab72999; Abcam), anti-EZH2 (#612666; BD Biosciences), anti-ERα (#sc-543; Santa Cruz Biotechnology), anti-p300 (#A300-358A; Bethyl Laboratories), anti-CBP (#NB100-382; Novus Biologicals), anti-NCoR (#ab24552; Abcam), anti-HA (#901501; Biolegend), anti-H3K27me3 (#9733; Cell Signaling Technology), anti-GAPDH (#sc-365062; Santa Cruz Biotechnology), and anti-H3 (#ab1791; Abcam). Antibodies for ChIP assays include: anti-ERα (#sc-543; Santa Cruz Biotechnology and #MS-315; Thermo Scientific), anti-EZH2 (#39933; Active Motif), anti-H3K27me3 (#9733; Cell Signaling Technology), anti-p300 (#sc-48343X; Santa Cruz Biotechnology), anti-CBP (#ab2832; Abcam and #sc-7300; Santa Cruz Biotechnology), and anti-NCoR (#ab24552; Abcam). Antibodies used for IHC staining are mentioned below in the "IHC and quantification of IHC analysis" section. EZH2 inhibitors were purchased from Xcess Biosciences Inc. (GSK126, GSK343, and EPZ-6438). Estradiol (E2), tamoxifen metabolite 4-hydroxytamoxifen (4-OHT), and 5-Aza-2′-deoxycytidine (5-Aza) were obtained from Sigma, unless otherwise indicated.

Cell lines and transfection

Paired tamoxifen-sensitive and -resistant MCF-7, ZR-75-1, and T-47D cells were generated and provided by Dr. Rachel Schiff at Baylor College of Medicine (Houston, TX; refs. 16, 17). The parental MCF-7 was obtained from Dr. Marc Lippman at the National Cancer Institute (Bethesda, MD); ZR-75-1 and T-47D were purchased from ATCC. Authenticity of each cell line was confirmed once the resistance to tamoxifen was established. siRNA was transfected using Lipofectamine 2000 transfection reagent (Invitrogen) following the manufacturer's instruction. Stable clones were selected and maintained in either 2 μg/mL of puromycin (Sigma) for shRNAs or 200 μg/mL of Hygromycin B (Sigma) for EZH2 overexpression.

Quantitative RT-PCR

Total RNA was isolated using TRIzol Reagent (Invitrogen) and subjected to RT-PCR using High-Capacity cDNA Reverse Tran-

scription Kit (Thermo Fisher Scientific). Gene expression was calculated as described previously (15), and primers used for qPCR are listed in the Supplementary Table S1.

Chromatin immunoprecipitation assay

Chromatin immunoprecipitation (ChIP) was performed as described previously (15). Quantitative PCR was then performed with specific primers of targeted sites, the sequences of which are listed in Supplementary Table S2. Details are described in the Supplementary Materials and Methods.

RNA-Seq data analysis

RNA-Seq libraries were constructed using TruSeq RNA Sample Prep Kit v2 (Illumina, #RS-122-2001), and then sequenced on HiSeq 3000 at Genome Sequencing Facility of The University of Texas Health Science Center at San Antonio (UTHSCSA, San Antonio, TX). The sequencing reads were aligned to human genome (hg19) using TopHat 2.0.10 (Bowtie2 2.1.0), and edgeR 3.12.1 was used to call differentially expressed genes. Data analyses were detailed in the Supplementary Materials and Methods.

Gene signature definition

Genes differentially expressed upon silencing of EZH2 were overlapped with chemical and genetic perturbations (CGP) gene sets from C2-curated category in MSigDB dataset collection (18). The P values were calculated on the basis of the hypergeometric distribution, and the top 100 enriched gene sets were selected for the following analysis. To determine the gene signatures that were coregulated by EZH2 and ERα signaling, ERα-dependent core genes were first defined by the following two criteria: (i) expression of these genes were significantly changed upon E2 stimulation, and (ii) each gene contains at least one ERα binding peak within 30 kb from its transcription start site (TSS) in MCF-7 cells. ERα ChIP-Seq data were retrieved from GSE25710 (19), and binding peaks were called by MACS with default parameters (20). Genes that were shared between ERα-dependent core genes and EZH2-regulated ones were identified as the signature genes that are controlled by both EZH2 and ERα signaling.

Patient information

In this study, 130 paraffin-embedded tissue samples were included and collected from patients with ERα-positive, stage 0–II breast cancer. Patient cohorts for IHC staining, tumor specimen collection, survey data, and all clinical and pathologic information were reviewed and approved by the Review Board on Human Research of Universidad de La Frontera, Hospital de Temuco (Chile). Protocols of the study were approved by the Ethic Committees of the participating institutions (Universidad de la Frontera and Instituto de Biología y Medicina Experimental). This study was conducted under the provisions of the Declaration of Helsinki and informed written consents were obtained from all patients before inclusion. Pretreatment staging of the selected patients was classified according to the American Joint Committee on Cancer (AJCC) staging system (21) and the Elston and Ellis histologic grading system (22). Clinical pathologic data of the cohorts are shown in Supplementary Table S3.

IHC analysis and quantification

Paraffin-embedded breast cancer samples from patients and xenograft tumors were subjected to IHC staining with primary antibodies as follows: EZH2 (dilution 1:200; #NCL-L-EZH2;

Novocastra), GREB1 (dilution 1:400; #MABS62; EMD Millipore), ERα (dilution 1:75; #NCL-L-ER-6F11; Novocastra), Ki67 (dilution 1:400; #9027; Cell Signaling Technology), and cleaved caspase-3 (dilution 1:100, #9661S; Cell Signaling Technology). The expression levels of EZH2, GREB1, and ERα were assessed using a combination of both intensity and proportion of stained cells with different criteria according to the method described previously, respectively (2, 23–25). Details of quantification of staining are described in the Supplementary Materials and Methods.

For correlation analysis, all the samples were stratified into three groups based on IHC scores of either EZH2 or ERα (low, scores of EZH2 $\leq$3 or scores of ERα $= 1$; medium, 3< scores of EZH2 $\leq$6 or scores of ERα $= 2$; high, scores of EZH2 >6 or scores of ERα $= 3$). Afterwards, the distribution of each GREB1 IHC score within one particular group was calculated. *P* values were obtained by Fisher exact analysis.

DNA methylation data analysis and pyrosequencing assay

Illumina HumanMethylation450K BeadChip data for parental MCF-7 and three MCF-7–derived, endocrine-resistant cell lines were retrieved from GSE69118 (26). Raw data were preprocessed and background normalized with the Bioconductor package minfi as described previously (27). Genome-wide DNA methylome in TCGA was retrieved from Firehose (28). Only those samples that were collected from ER$^+$ patients and have both DNA methylation and mRNA-Seq data available were retained. Any methylation probes with more than 50 missing data were excluded.

Distribution of the pathologic stages of breast cancer in TCGA cohort regarding the involvement of regional lymph nodes was plotted on the basis of the average methylation levels at three probes that show the strongest negative correlation with *GREB1* expression. Patients were stratified into four groups according to the average methylation levels at those three probes, distribution of each pathologic staging classification among these groups was then compared using Fisher exact test.

Five-hundred nanograms of genomic DNA per sample was bisulfite converted using the EZ DNA Methylation Kit (Zymo Research) according to the manufacturer's instruction. The methylation levels were quantified by the PyroMark Q96 MD System at the Bioanalytics and Single-Cell Core (BASiC) of UTHSCSA. The methylation percentage of each interrogated CpG site was calculated by PyroMark CpG software (Qiagen). Details of primer sequence and pyrosequencing assay are described in the Supplementary Materials and Methods.

In vivo studies

All the animal work was performed with the approval of UTHSCSA Institutional Animal Care Committee and the animals were handled in accordance with institutional and national guidelines for animal experiments. Briefly, 5×10^6 TamR MCF-7 cells were mixed with equal volume of Matrigel (Thermo Fisher Scientific), and then injected subcutaneously into the inguinal mammary fat pads of 6-week-old female nude mice (Charles River) at both sides. Estrogen pellets (Innovative Research, 0.72 mg 60-day release) were implanted on the same day of cell inoculation. When tumors reached the volume of approximately 200–300 mm^3, mice were randomly assigned into either treatment group or control group. 4-Hydroxytamoxifen (Tocris Bio-

science) was given subcutaneously at a dose of 100 μg per mouse every day. The powder of EZH2 inhibitors was dissolved in 20% captisol (CyDex Pharmaceuticals, Inc.). GSK126 was administered intraperitoneally while EPZ-6438 was by oral gavage. Both drugs were delivered either daily for 5 days per week at 50 mg/kg dose or twice per week at 300 mg/kg dose. The captisol vehicle was administered into the control animals with the same volume of 200 μL per mouse. Tumor sizes were measured with calipers and body weights were monitored twice weekly throughout the experiment. Tumors from each group were harvested after 35 days of treatment, and then snap frozen in liquid nitrogen or fixed in 10% formalin for downstream studies.

Accession number

The RNA-Seq data of EZH2 knockdown in TamR MCF-7 cells and EZH2 overexpression in MCF-7 cells were deposited at the Gene Expression Omnibus database with an accession number GSE103243.

Results

EZH2 renders tamoxifen resistance in breast cancer cells

In the publicly available gene expression datasets from ER$^+$ breast cancer patients who received tamoxifen as an adjuvant treatment (29, 30), we observed a dramatic increase of EZH2 transcript level in clinical samples that are resistant to tamoxifen compared to the sensitive ones (Fig. 1A; Supplementary Fig. S1A). Higher level of EZH2 was significantly associated with poorer disease-free survival in these patients (Fig. 1B; Supplementary Fig. S1B). These results suggest that EZH2 may play an important role associated with drug resistance in breast cancer.

To explore the exact biological effects of EZH2 in acquired treatment resistance, we overexpressed EZH2 in tamoxifen-sensitive, ER$^+$ breast cancer MCF-7 cells (Fig. 1C) or knocked down EZH2 in MCF-7–derived, TamR cells (Fig. 1D), and then measured cellular response to increasing concentrations of 4-hydroxytamoxifen (4-OHT), the active metabolite of the antiestrogen. Although overexpression of EZH2 led to decreased sensitivity of MCF-7 to tamoxifen (Fig. 1C), depletion of EZH2 attenuated the agonistic effect of tamoxifen on TamR cell proliferation (Fig. 1D). This result was also confirmed in TamR counterpart of another ER$^+$ breast cancer cell line, TamR ZR-75-1 (Supplementary Fig. S1C). Collectively, these results indicate that EZH2 is essential for conferring tamoxifen resistance and represents a promising therapeutic target. Therefore, we tested two EZH2 inhibitors (GSK343 and EPZ-6438) that selectively block its methyltransferase activity in three ER$^+$ TamR breast cancer cell lines (TamR MCF-7, TamR ZR-75-1, and TamR T-47D) and found that both drugs dramatically suppressed cell growth (Fig. 1E; Supplementary Fig. S1D and S1E), suggesting that inhibition of EZH2 enzymatic activity is a putative approach to treating endocrine therapy–resistant breast cancer.

EZH2 orchestrates an ERα-dependent transcriptional program in favor of endocrine resistance

The role of EZH2 in controlling cell sensitivity to tamoxifen made us wonder whether ERα activity in the presence of tamoxifen could be regulated by EZH2. To this end, we performed RNA-Seq after knocking down EZH2 in TamR MCF-7 cells. Gene set enrichment analysis (GSEA) of genes that were

Wu et al.
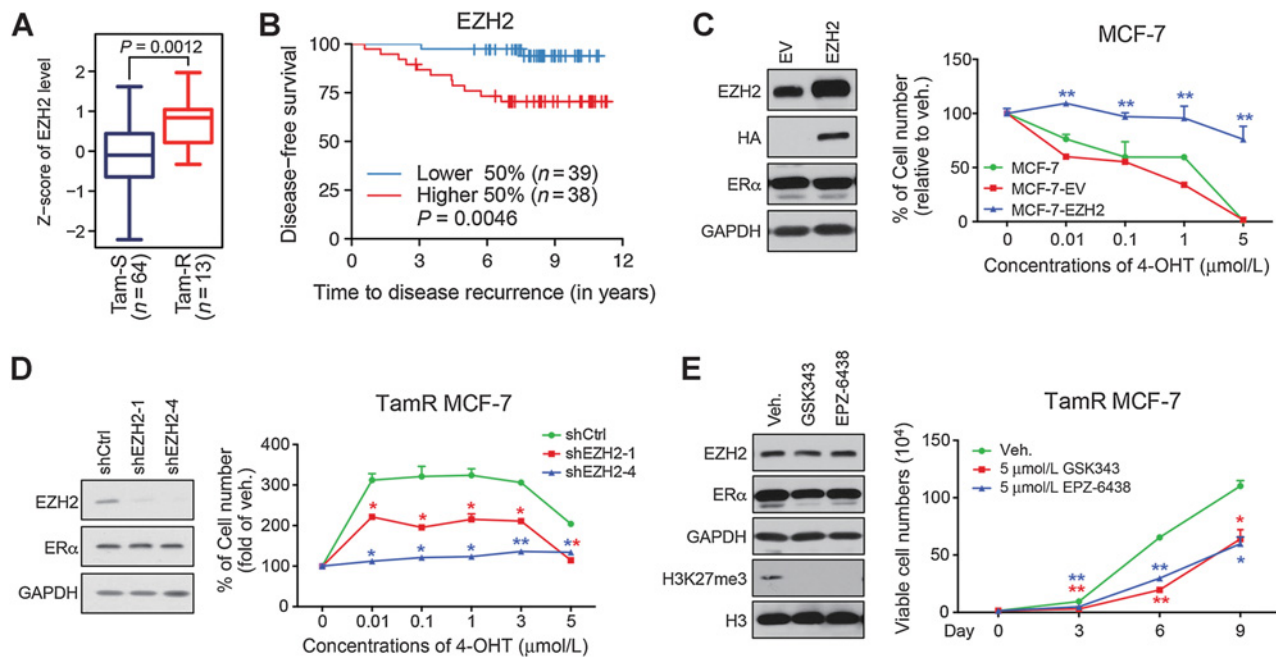
Figure 1.
EZH2 confers tamoxifen resistance in breast cancer cells. **A** and **B,** Comparison of EZH2 mRNA level in breast tumors according to their sensitivities to tamoxifen (**A**) and Kaplan–Meier analysis (**B**) of disease-free survival based on EZH2 mRNA levels using GSE9195 cohort (29). Tam-R, tamoxifen-resistant; Tam-S, tamoxifen-sensitive. Red curve, top 50% with high EZH2 level; blue curve, bottom 50% with low EZH2 level. N in brackets, number of patients in each specific group. P value was calculated by Mann–Whitney test (**A**) and log-rank test (**B**). **C** and **D,** Responses to tamoxifen in originally sensitive MCF-7 cells upon no transfection (MCF-7), stably expressing either empty vector (MCF-7-EV) or HA-tagged EZH2 (MCF-7-EZH2; **C**) and in TamR MCF-7 cells with EZH2 depletion using two independent shRNAs (shEZH2-1 and -4; **D**). Cell numbers were counted after 7 days of incubation with indicated concentrations of 4-OHT. Left, Western blot analysis of total cell lysates with indicated antibodies. **E,** Inhibitory effect of EZH2 inhibitors (GSK343 and EPZ-6438) on proliferation of TamR MCF-7 cells. Cells were maintained in 100 nmol/L 4-OHT and treated with DMSO (Veh.), 5 μmol/L GSK343 or EPZ-6438, then collected at indicated time points for cell counting. Left, Western blot analysis of total cell lysates and nuclear extract. Data were presented as mean ± SEM of triplicates. *, $P < 0.05$; **, $P < 0.001$, and P values in **C–E** were calculated by two-tailed t test.

differentially expressed upon EZH2 silencing revealed that ERα-regulated genes were significantly enriched (Fig. 2A). To our surprise, when we compared these EZH2-dependent genes with those differentially expressed upon hormone treatment in MCF-7, we found that EZH2 depletion in TamR cells resulted in a transcriptional profile highly similar to the gene expression pattern prompted by tamoxifen in parental cells (Fig. 2B). This intriguing observation indicates that loss of EZH2 switches the transcriptional regulatory network in TamR MCF-7 cells back to the one sensitive to the antiestrogen. To further prove the conclusion, gene expression profiling was also carried out in EZH2-overexpressing MCF-7 cells (Fig. 2C). Interestingly, responses of tamoxifen-regulated genes to the endocrine agent were all alleviated, or say muted, when EZH2 was overexpressed (Fig. 2C; Supplementary Fig. S2A), suggesting that overabundance of EZH2 makes tamoxifen-sensitive breast cancer cells refractory to the drug. In addition, we found gene signatures that are involved in endocrine resistance development were highly represented in the functional categories of EZH2-regulated genes (Fig. 2D), especially those that were upregulated upon EZH2 knockdown (Supplementary Fig. S2B), highlighting the transcriptional repression function of EZH2 in endocrine resistance.

To elucidate how EZH2 functionally regulates ERα activity responding to tamoxifen precisely, we detected the expression changes of four classical ERα target genes upon modulation of

EZH2 levels in the presence of 4-OHT. Expression of these ERα targets was no longer inhibited, or even increased, when EZH2 was overexpressed in MCF-7 (Fig. 2E), although was suppressed upon EZH2 silencing in the resistant TamR cells (Fig. 2F) by tamoxifen. ERα binding to the *cis*-regulatory elements near these ERα targets was somewhat increased or generally comparable when EZH2 was overexpressed (Fig. 2G; Supplementary Fig. S3A) or knocked down (Fig. 2H; Supplementary Fig. S3B). Interestingly, in MCF-7 cells with overabundance of EZH2, the recruitment of ERα coactivators p300 and CBP were significantly elevated, and the binding of NCoR, a corepressor that mediates the antagonistic effects of tamoxifen (31), was dramatically decreased (Fig. 2G; Supplementary Fig. S3A). In contrast, in TamR MCF-7 that was depleted of EZH2, recruitment of p300 and CBP to these ERα target loci was diminished, whereas NCoR bound with much stronger intensities (Fig. 2H; Supplementary Fig. S3B). All of these results indicate that EZH2 reprograms an ER-dependent transcriptional network that retains transactivation functioning even in the presence of tamoxifen. However, occupancy of ERα and its coregulators at ERα-binding elements near E2-stimulated genes that were not regulated by EZH2 were similar or marginally changed, no matter how EZH2 protein levels were manipulated (Supplementary Fig. S3C and S3D). This result suggests that EZH2 regulates the functional composition of ERα-associated transcriptional complex at specific ERα-bound regulatory regions rather than in a global, general way. Transcript levels of *ESR1*, *p300*, *CBP*,
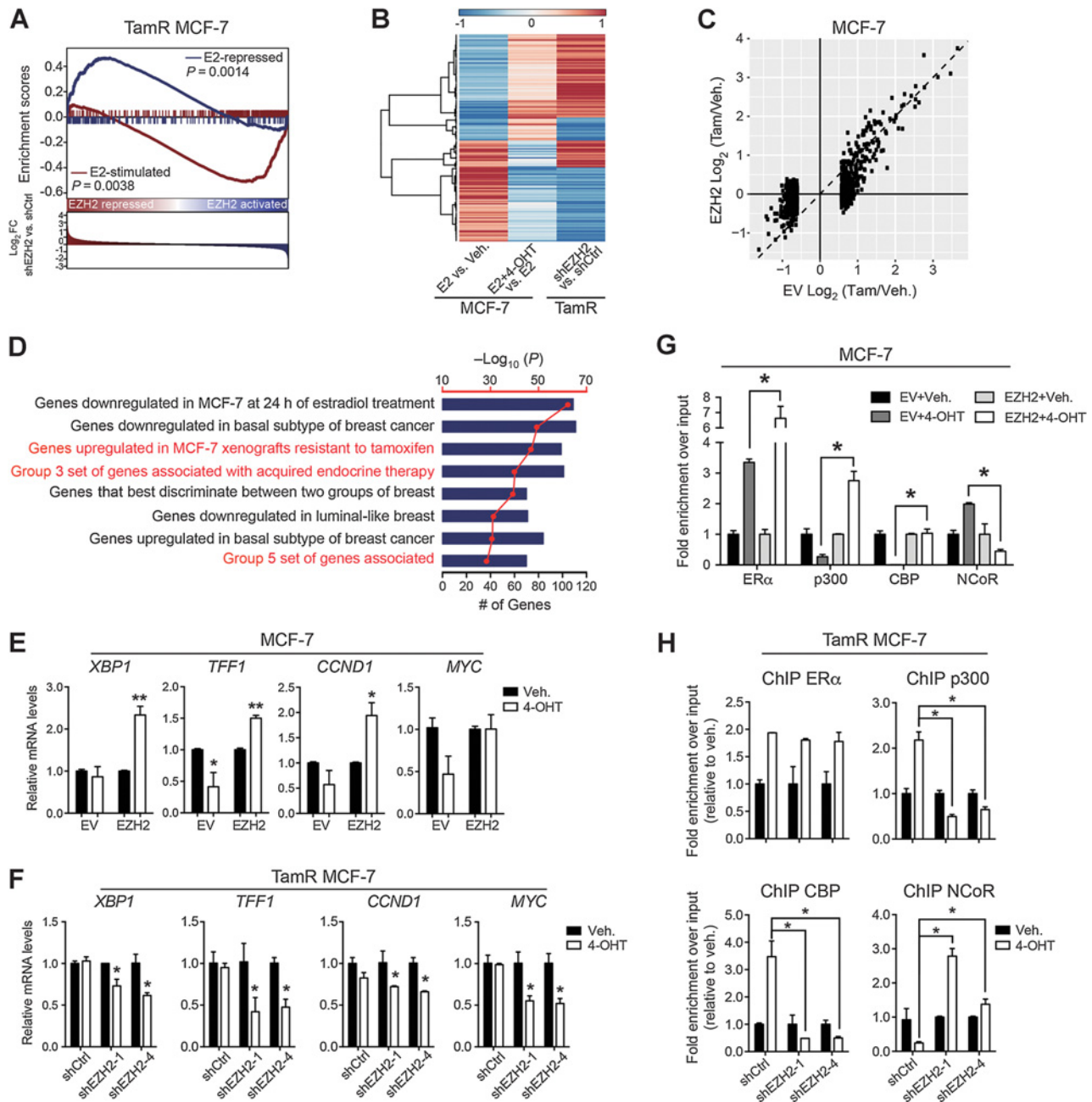
Figure 2.
EZH2 regulates an ERα-associated transcriptional profile in favor of endocrine resistance. **A,** GSEA analysis of differentially expressed genes upon EZH2 knockdown in TamR MCF-7 cells. *P* values were determined by Kolmogorov–Smirnov test. **B,** Unsupervised hierarchical cluster analysis of genes that were changed when MCF-7 was treated with E2 (E2 vs. Veh.) or E2 plus 4-OHT (E2 + 4-OHT vs. E2) using GSE25316 dataset (19) and genes that are differentially expressed upon EZH2 knockdown in TamR MCF-7 cells (shEZH2 vs. shCtrl). Color scale bar indicates the $\log_2$ of differential gene expression from the lowest (blue) to the highest (red) level. **C,** Scatter plot showing transcriptional changes of tamoxifen-regulated genes upon the antiestrogen treatment (fold change ≥ 1.5, $P_{adj} < 0.05$) in either control cells (*x*-axis) or EZH2-overexpressing MCF-7 cells (*y*-axis). **D,** Functional annotations of EZH2-regulated genes in TamR MCF-7 cells. Annotations that are associated with endocrine therapy resistance were highlighted in red. Blue bar, numbers of genes overlapped within each indicated gene set; red line, adjusted *P* value of each functional category. **E** and **F,** Quantitative RT-PCR showing expression changes of ERα target genes in MCF-7 cells upon EZH2 overexpression (**E**) and TamR MCF-7 cells upon EZH2 depletion (**F**) with the treatment of either ethanol (Veh.) or 100 nmol/L 4-OHT for 6 hours. **G** and **H,** ChIP-qPCR results at *cis*-regulatory elements near *XBP1* gene in EZH2-overexpressing MCF-7 cells (**G**) and EZH2-silenced TamR MCF-7 cells (**H**) with the treatment of 1 μmol/L 4-OHT for 45 minutes. Data were plotted as means ± SEM of replicates after being normalized to *GAPDH* (mRNA) or KIAA0066 (ChIP-qPCR) as the internal control. *, $P < 0.05$ and **, $P < 0.001$ by two-sided *t* test.

and *NCoR* were controlled by neither tamoxifen treatment nor EZH2 (Supplementary Fig. S4A and S4B). Protein levels of these transcription (co)factors were marginally altered as well, except that p300 and CBP proteins seemed to be increased upon EZH2 knockdown in the presence of 4-OHT (Supplementary Fig. S4C). Collectively, these findings indicate that EZH2 recomposes an ERα-centered transcriptional complex in the presence of tamoxifen and therefore reprograms the ERα-dependent gene expression profiles, which potentially leads to the refractory phenotype in breast cancer cells.

EZH2 epigenetically silences ERα cofactor GREB1

Our above analysis indicates that EZH2 renders tamoxifen resistance by regulating ERα activity in response to the antagonist. Because ERα protein was barely changed upon manipulation of EZH2 level or enzymatic activity, this raises the possibility that EZH2 may actually modulate an ERα-regulatory protein that controls cell response to tamoxifen. Thus, we first defined a list of genes that are regulated by EZH2 and estradiol, contain at least one ERα binding peak around their TSSs and are functionally related to endocrine resistance. 43 genes were thus filtered out, and expression of each individual gene was associated with tamoxifen responses in clinical samples by receiver operating characteristic (ROC) curve analysis (29, 30). As a control, EZH2 was spotted as the gene that is most significantly linked to tamoxifen resistance. Interestingly, one of the top upregulated genes upon EZH2 knockdown showing close correlation with tamoxifen sensitivity is *GREB1* (Fig. 3A), a well-known ERα cofactor (2). Similar result was obtained when all genes that were silenced by EZH2 were considered (Supplementary Fig. S5A).

To test whether *GREB1* is an EZH2-dependent target gene, we first knocked down EZH2 in TamR MCF-7 cells and detected a dramatic elevation of GREB1 at both transcript (Fig. 3B) and protein (Fig. 3C) levels. This result was further confirmed in TamR ZR-75-1 cells (Supplementary Fig. S5B and S5C). GREB1 protein was drastically increased upon the treatment of EZH2 inhibitors GSK343 and EPZ-6438 in all of the three tamoxifen-resistant cell lines we have (Supplementary Fig. S5D). It is notable that ERα levels were not significantly affected under any of the experimental conditions (Fig. 3B and C; Supplementary Fig. S5B–S5D). This implies that EZH2-mediated repression of GREB1 expression may be attributed to the enzymatic activity of the epigenetic regulator.

Therefore, we examined H3K27 trimethylation (H3K27me3) signal at *GREB1* promoter. EZH2 knockdown in TamR MCF-7 cells significantly diminished the intensity of H3K27me3 at two separate locations around *GREB1* TSS (Supplementary Fig. S6A). Decrease of H3K27me3 levels was also noticed near other EZH2-repressed genes in TamR cells upon EZH2 depletion (Supplementary Fig. S6B), suggesting that EZH2 is fully functional concerning regulation of the epigenetic mark H3K27me3. However, occupancy of both EZH2 and H3K27me3 were weak at *GREB1* promoter compared with well-characterized target locus such as *WNT1* promoter (Supplementary Fig. S6C; ref. 32) and the intensities of H3K27me3 were comparable between TamR and parental MCF-7 cells (Supplementary Fig. S6C). These results indicate that H3K27me3 may not be the predominant epigenetic mark contributing to EZH2-mediated silencing of *GREB1* in endocrine-resistant breast cancer cells. Considering an important role of EZH2 in dictating DNA methylation, we

next examined whether methylation of any CpG sites at *GREB1* promoter is functionally important and can be modulated by EZH2. We first retrieved genome-wide methylation profiles in MCF-7 and three different endocrine-resistant counterpart cell lines (26), and then inspected the DNA methylation levels near or within *GREB1* gene. Strikingly, we located a CpG-containing area at *GREB1* promoter showing remarkably strong methylation in all of these three endocrine-resistant cells, but very minimal signals in the parental MCF-7 (Fig. 3D, top). When we examined the DNA methylation pattern of the entire *GREB1* gene in TCGA methylome data from ER$^+$ breast cancers (28), we found that DNA methylation signals at this particular locus showed strong negative correlation with *GREB1* expression (Fig. 3D, middle). More interestingly, we obtained a significant, positive association between pathologic statuses concerning nearby lymph node involvement, one of the most informative factors evaluating tumor progression, and DNA methylation signals at the subloci that show the strongest negative correlation with *GREB1* levels (Fig. 3D, bottom). Moreover, the transcript level of *GREB1* was significantly decreased in patients' samples resistant to tamoxifen therapy in two independent cohorts (Supplementary Fig. S6D and S6E), which was notably associated with poorer disease-free survival (Supplementary Fig. S6F and S6G). Taken together, these results suggested the important role of GREB1 in endocrine resistance, which may be attributed to DNA methylation at its promoter region.

We next asked whether EZH2 could control DNA methylation at this specific site. Pyrosequencing analysis showed a significant decrease of DNA methylation in TamR MCF-7 cells upon EZH2 knockdown compared with the control (Fig. 3E). Similarly, EZH2 overexpression in the parental MCF-7 cells induced nearly 2-fold increase in DNA methylation signals at *GREB1* promoter region, although it was not statistically significant possibly due to the extremely low basal methylation signal (Supplementary Fig. S6H). Furthermore, EZH2 overexpression–induced silencing of *GREB1* gene in MCF-7 cells was relieved by the DNA methyltransferase (DNMT) inhibitor 5-Aza-2′-deoxycytidine (5-Aza; Fig. 3F), whereas EZH2 depletion plus 5-Aza treatment in TamR cells led to the most dramatic increase in *GREB1* mRNA levels (Fig. 3G). All these results indicate that EZH2-mediated suppression of *GREB1* expression is conceivably mediated through DNA methylation. It is worthy of note that our gene expression profiling in TamR MCF-7 cells identified DNA methyltransferases *DNMT1* and *3B* as two significantly downregulated genes upon EZH2 depletion (Supplementary Fig. S6I). This may give an explanation for the dependency of DNA methylation signals on EZH2 at *GREB1* promoter region.

GREB1 recomposes ERα-associated transcriptional complexes responding to different ligands

We then sought to understand the exact role of GREB1 in orchestrating ERα activity in response to the antiestrogen. GREB1 was silenced in MCF-7 cells treated with estradiol and/or 4-OHT (Fig. 4A). Efficient knockdown of GREB1 drastically decreased E2-stimulated expression of ERα target genes (Fig. 4B). This is in line with previous report that GREB1 is essential for estrogen-specific activation of ERα signaling (2). In contrast, expression of these genes was no more suppressed and even enhanced by tamoxifen when GREB1 was depleted (Fig. 4B).
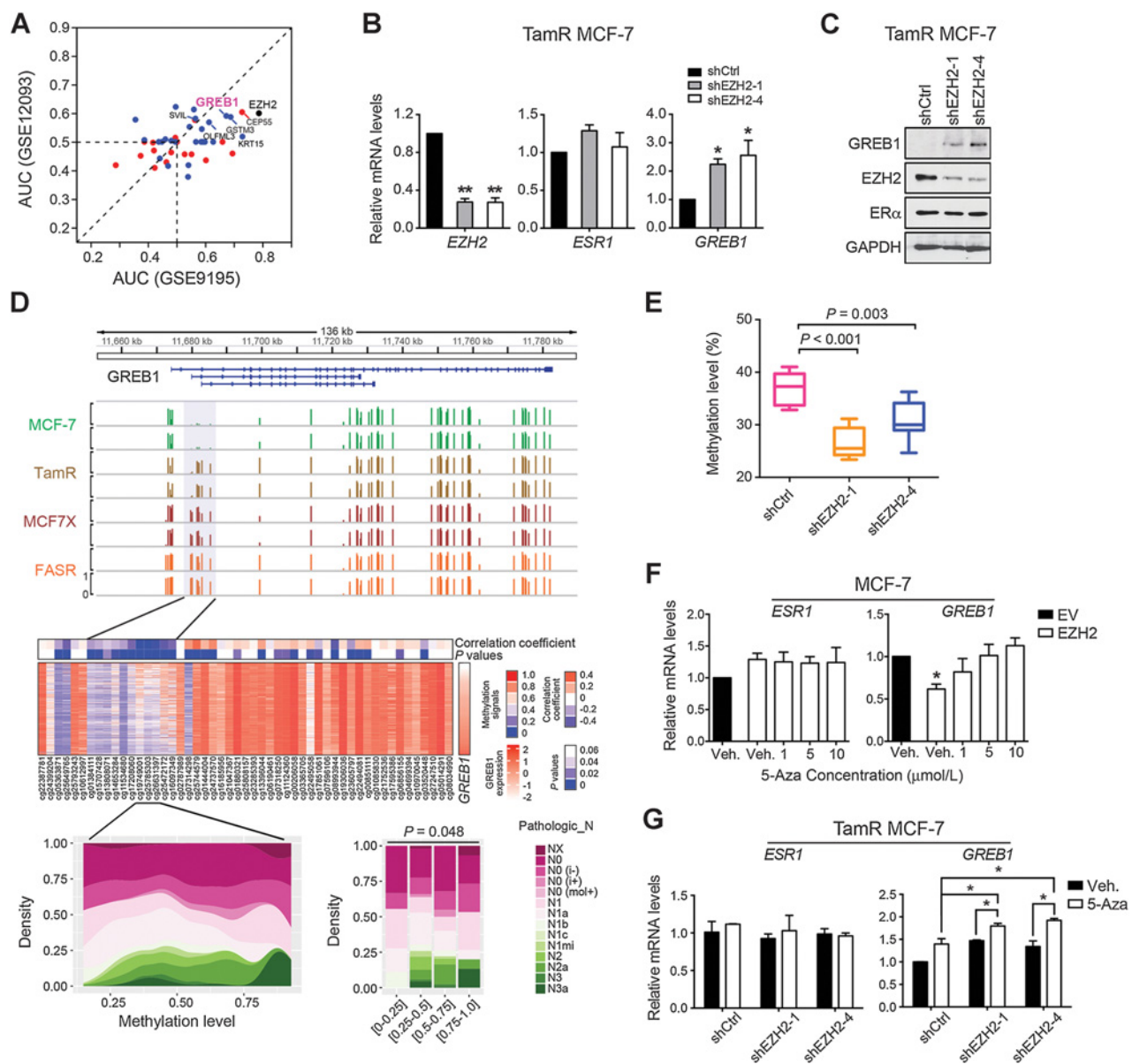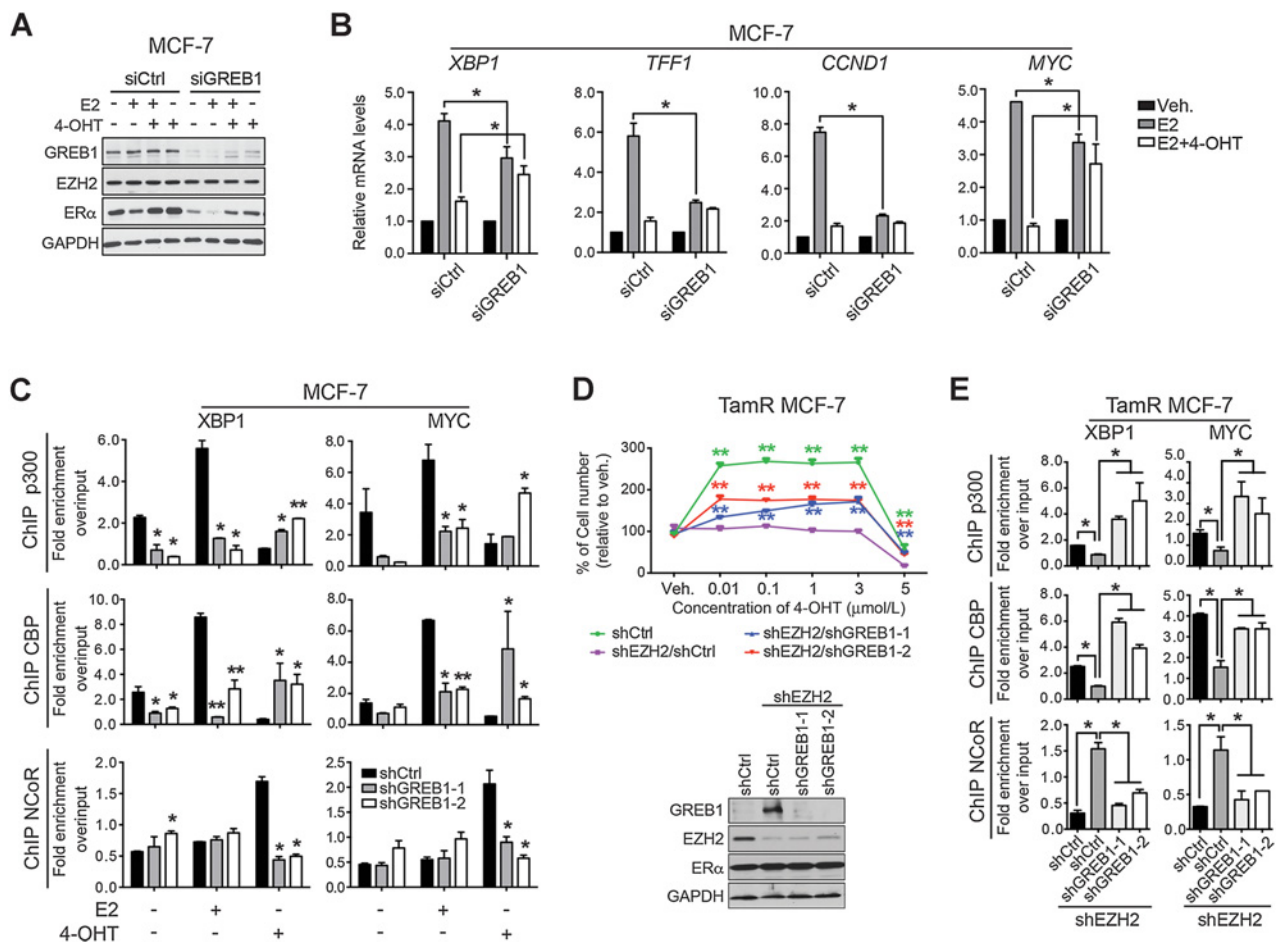
Figure 3.
EZH2 epigenetically silences GREB1 expression via DNA methylation. **A,** ROC curve analysis indicating the correlation of EZH2-regulated genes that are involved in ERα signaling with tamoxifen responses in GSE9195 and GSE12093 cohorts (29, 30). Blue dots, EZH2-repressed genes; red dots, EZH2-activated genes. **B** and **C,** Upregulation of GREB1 at both mRNA (**B**) and protein (**C**) levels upon shEZH2 in TamR MCF-7 cells. **D,** Clinical relevance of DNA methylation at a specified area within *GREB1* promoter. Top, duplicates of DNA methylation profiling in MCF-7 cells and three distinct endocrine-resistant, MCF-7–derived cell lines (26). TamR, tamoxifen-resistant; MCF7X, estrogen deprivation resistant; FASR, fulvestrant resistant. Location of the CpG sites displaying differential patterns is highlighted in gray. Middle, heat map depicting the correlation of DNA methylation signals at each specified probe for every single patient with *GREB1* expression in TCGA data (28). Bottom, correlation between the methylation levels of the underlined probes with pathologic stages concerning the involvement of regional lymph node. *P* value was calculated by Fisher exact test. **E,** Decrease in DNA methylation intensity at *GREB1* promoter region upon EZH2 depletion in TamR MCF-7 cells. Pyrosequencing was performed at locus highlighted in **D**. **F,** Restoration of EZH2 overexpression-induced repression of *GREB1* expression by 5-Aza. Control (EV) or EZH2-overexpressing (EZH2) MCF-7 cells were treated with DMSO (Veh.) or increasing concentrations of 5-Aza (1, 5, and 10 μmol/L) for 72 hours. **G,** RT-qPCR showing transcript levels of *GREB1* and *ESR1* upon EZH2 knockdown with or without 5-Aza treatment. Stable TamR MCF-7 clones were treated with DMSO (Veh.) or 5-Aza (5 μmol/L) for 120 hours. Data are presented as means ± SEM of replicates. *, $P < 0.05$ and **, $P < 0.001$ by two-sided *t* test.

It has been reported that GREB1 conciliates interaction between ERα and other cofactors at targeted *cis*-regulatory chromatin regions (2), so we next investigated whether GREB1 modulates the hierarchical structures of ERα-associated tran-

scriptional complex responding to different ligands. Upon estradiol treatment, recruitment of ERα coactivators p300 and CBP were dramatically decreased by GREB1 depletion, which is in agreement with published data (Fig. 4C; ref. 2). In the

Wu et al.

Figure 4.
GREB1 blocks the activation of tamoxifen-liganded ERα. **A** and **B,** Alleviation of the inhibitory effects of tamoxifen on ERα activity upon GREB1 knockdown. Upon transient transfection with control siRNA (siCtrl) or siRNA pool targeting GREB1 (siGREB1), MCF-7 cells were hormone deprived for 3 days and then treated with ethanol (Veh.), 10 nmol/L E2, or 10 nmol/L E2 plus 100 nmol/L 4-OHT for 6 hours. Total cell lysates were prepared for immunoblotting (**A**) or total RNA was subjected to qRT-PCR (**B**). mRNA levels were normalized to *GAPDH* and are presented as mean ± SEM of replicates. **C,** Binding of ERα coregulators near target genes in GREB1-depleted breast cancer cells. GREB1 was silenced in MCF-7 cells by two independent shRNAs (shGREB1-1 and shGREB1-2), and the stable clones were treated with ethanol (Veh.), 100 nmol/L E2, or 1 μmol/L 4-OHT for 45 minutes after hormone deprivation for 3 days. Quantitative PCR was performed and are presented as mean ± SEM of replicates. **D,** Essential role of GREB1 in mediating the effects of EZH2 on conferring resistance to tamoxifen. Stable clones of EZH2-depleted (shEZH2) TamR MCF-7 cells were infected with two independent shGREB1 and treated with 4-OHT at indicated concentrations for 7 days before cell numbers were counted. Bottom, Western blot analysis confirming the knockdown efficiencies of shEZH2 and shGREB1. Statistical difference was calculated in comparison with the data from EZH2-depleted cells. **E,** ChIP-qPCR showing reverse of EZH2 depletion-induced chromatin redistribution of ERα coregulators upon GREB1 knockdown. Data are presented as mean ± SEM of triplicates. *, $P < 0.05$ and **, $P < 0.001$ by two-tailed t test.

presence of 4-OHT, however, silencing of GREB1 led to significantly increased intensity of p300 and CBP at these ERα binding. Coincidentally, the presence of NCoR was diminished (Fig. 4C). All these results suggest a novel and critical function of GREB1 in refining proper compositions of ERα-centered transcriptional complexes in response to different ligands. Functionally, knockdown of GREB1 in MCF-7 impaired E2-stimulated cell growth, but reversed the inhibitory effect of 4-OHT and even promoted cell proliferation in the presence of the antiestrogen (Supplementary Fig. S7A). As such, GREB1-depleted MCF-7 cells survived after 7 days of incubation with 4-OHT even at concentration as high as 5 μmol/L, under which condition the control cells stopped growing and underwent apoptosis (Supplementary Fig. S7B).

Next we asked whether the role of EZH2 in recomposing ERα-centered transcriptional complex in response to tamoxifen is actually mediated by the modulatory function of GREB1 on ERα activity. Therefore, we knocked down GREB1 in EZH2-depleted TamR MCF-7 cells by two independent shRNAs against GREB1 (Fig. 4D, bottom). We first examined how cells responded to tamoxifen. As what we observed previously, knockdown of EZH2 alone abolished the stimulating effect of tamoxifen on cell growth (Figs. 1D and 4D; Supplementary Fig. S1C). When GREB1 was depleted simultaneously, however, the double-knockdown cells became refractory to tamoxifen again (Fig. 4D, top). At selected ERα-binding sites, EZH2 depletion led to decreased intensities of p300 and CBP but increased recruitment of NCoR in TamR cells (Fig. 4E). However, chromatin binding of these regulatory

proteins reversed back to the original levels when GREB1 was concurrently depleted. Notably, binding intensities of p300 and CBP at the selected sites were in general higher when both EZH2 and GREB1 were knocked down than in the control cells (Fig. 4E), which may be explained by the increased protein levels of p300 and CBP upon 4-OHT treatment in EZH2-depleted TamR cells (Supplementary Fig. S4C). These results suggest that reprogramming of ERα-involved transcriptional network in resistant cells, which is orchestrated by EZH2, requires the maintenance of GREB1 protein at low levels. Otherwise, GREB1 reallocates ERα cofactors to *cis*-regulatory elements to ensure proper inactivation of ERα signaling responding to the antiestrogen.

Pharmacologic inhibition of EZH2 retarded the growth of xenograft tumors in TamR mouse model

To explore the translational potential of our findings, we evaluated the efficacy of two EZH2 inhibitors, GSK126 and EPZ-6438 (13, 33), in a TamR xenograft mouse model. Both EZH2-targeting compounds started to suppress the sizes of TamR MCF-7 xenograft tumors markedly after 2 weeks of administration, and retained the inhibitory effects throughout the entire treatment period (Fig. 5A). No differences in animal body weights were observed between control and treatment groups, indicating that GSK126 and EPZ-6438 were well tolerated by mice (Fig. 5B). A histopathologic characterization of the xenograft tumors showed a decreased Ki67 labeling and relatively higher signal of cleaved caspase-3 in tumors from treatment groups, implying a reduced proliferation rate and potentially enhanced apoptosis (Fig. 5C). Immunoblot analysis of extracts from four independent xenograft tumors in either control or treatment groups confirmed that GREB1 protein was notably elevated by EZH2 inhibitors, whereas ERα and EZH2 were marginally changed (Fig. 5D, top). The result was better illustrated by the quantification of each protein level in
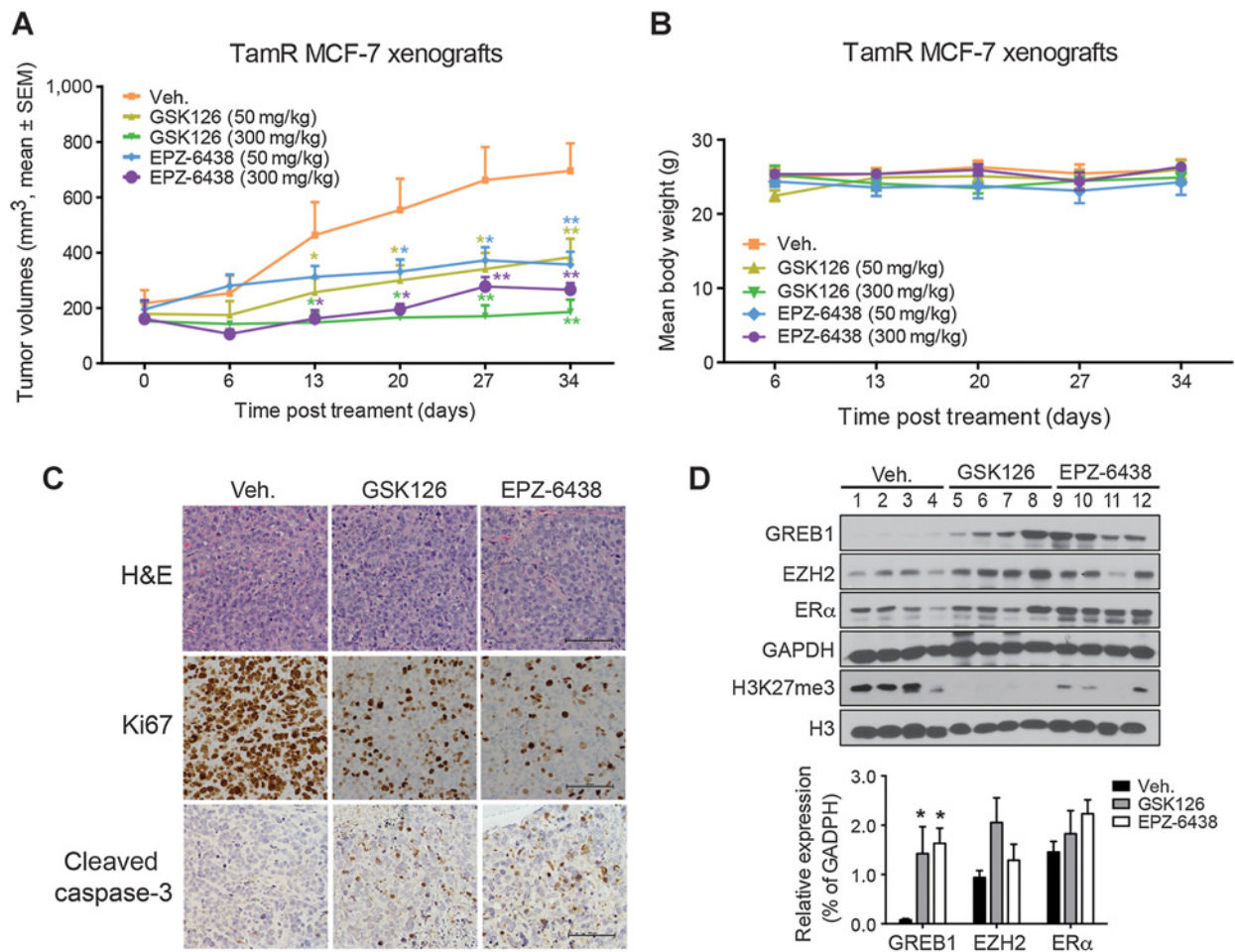

Figure 5.
Pharmacologic inhibition of EZH2 represents a promising therapeutic strategy for TamR breast cancer. **A,** Efficacy of EZH2 inhibitors on the growth of TamR xenograft tumors at the indicated dose for a course of 35 days. Data are presented as mean tumor volume ± SEM. **B,** Effects of EZH2 inhibitors on body weights of mice receiving the treatment. Data are presented as mean ± SEM. **C,** Characterization of TamR MCF-7 xenograft tumors with histologic analysis by hematoxylin and eosin (H&E) staining and IHC staining of Ki67 and cleaved caspase-3. Scale bars, 100 μm. **D,** Western blot analysis of indicated proteins in TamR xenograft tumors. Bottom, quantitative densitometry of protein levels of GREB1, EZH2, and ERα. Number 1–12, numbers of randomly selected xenograft tumors with four individual samples per group. Data are presented as mean ± SEM. *, $P < 0.05$ and **, $P < 0.01$ by two-sided *t* test.

Wu et al.

quadruplicate samples (Fig. 5D, bottom). Taken together, these results suggest that EZH2 serves as a promising therapeutic target for TamR breast cancer and that pharmacologic inhibition of EZH2 potentially leads to derepression of GREB1 expression.

EZH2 and GREB1 negatively correlate with each other in ERα-positive breast cancer

Next we examined the association between levels of EZH2 and GREB1 in clinical scenarios. First, we correlated the expression of these two genes in transcriptional profiles from ER$^+$ breast cancer patients (28). We found that mRNA levels of *GREB1* and *EZH2* are inversely correlated, which became more prominent and significant when more percentages of samples

expressing high levels of *EZH2* were considered in the analysis (Fig. 6A). We then investigated the protein levels of EZH2 and GREB1 by IHC analysis in clinical tissues collected from ER$^+$ patients receiving adjuvant tamoxifen therapy. EZH2, GREB1, and ERα were specifically stained in tamoxifen-sensitive ($n = 108$) and TamR ($n = 22$) breast tumors, and the tissues were classified into four groups based on the staining intensities of EZH2 and GREB1 (Fig. 6B). Specificity of GREB1 antibody that was used for IHC analysis was validated in both MCF-7 cells and breast tumors (Supplementary Fig. S7C and S7D). Nuclear staining was predominantly observed, which was specifically diminished upon GREB1 silencing (Supplementary Fig. S7C) or in TamR samples (Supplementary Fig. S7D). These results prove that the signals this antibody recognizes
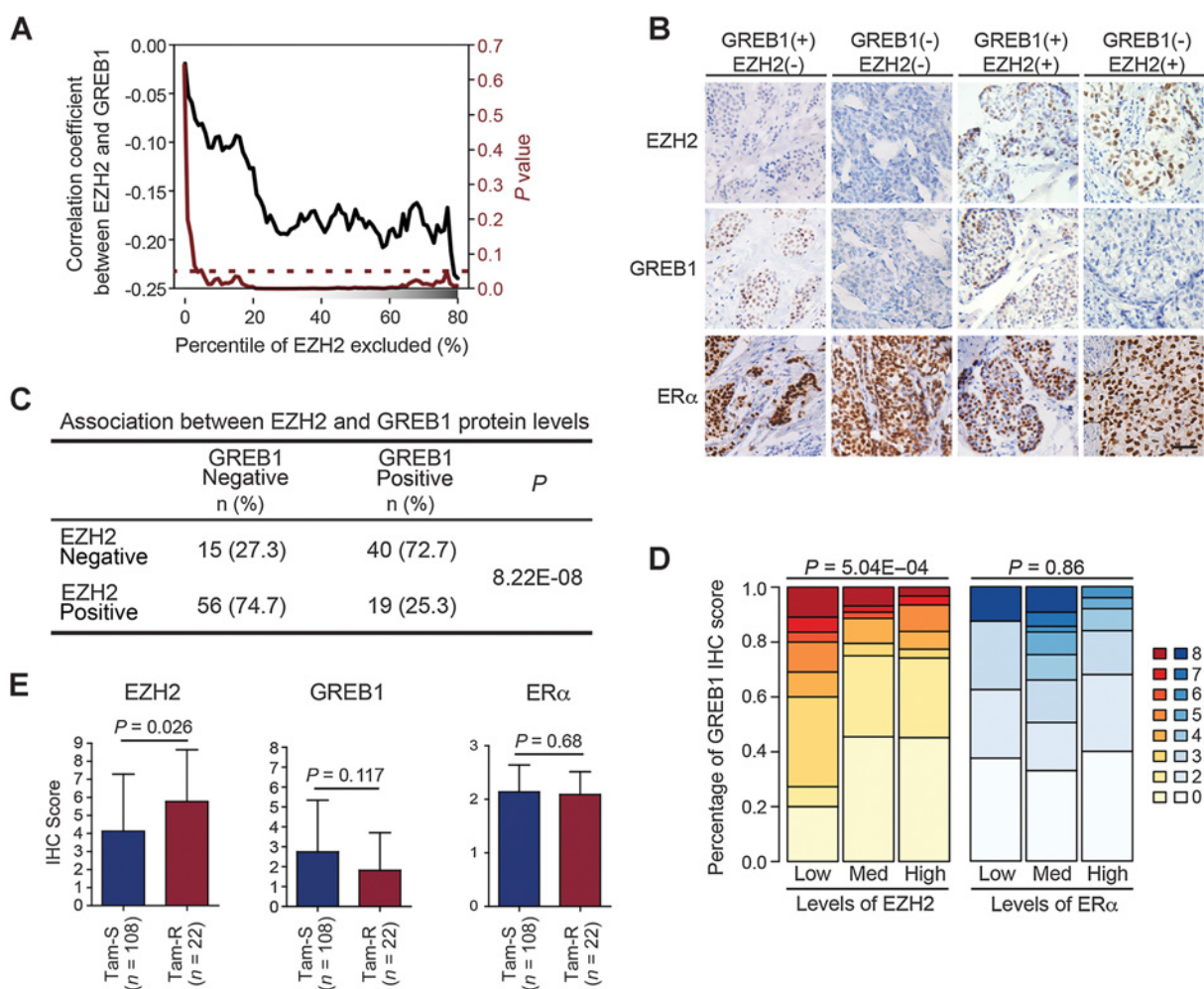
Figure 6.
Negative correlation between EZH2 and GREB1 in ER$^+$ breast cancer samples receiving tamoxifen as adjuvant treatment. **A,** Correlation between *EZH2* and *GREB1* transcript levels in patient samples. The black curve shows the correlation coefficients and the red shows the *P* value. The dotted red line represents *P* = 0.05. **B,** IHC staining showing nuclear staining of EZH2, GREB1, and ERα levels in representative ER$^+$ breast tumors. Scale bar, 50 μm. **C,** Correlation between EZH2 and GREB1 protein levels based on their IHC scores. *P* values were calculated using χ^2 analysis. **D,** Percentages of each GREB1 IHC score within the specific groups of samples that are stratified on the basis of either EZH2 (left) or ERα (right) IHC scores. Med, medium. *P* values were calculated using Fisher exact analysis. **E,** Quantification of EZH2, GREB1, and ERα IHC staining in tamoxifen-sensitive and TamR breast cancer patients. N in brackets, number of patients in each specific group. *P* values were determined by two-tailed Mann–Whitney test.

are indicative of a proper GREB1 isoform functioning as an ERα cofactor (2, 34). It is noteworthy that ERα levels were comparable among all the groups (Fig. 6B). In EZH2-positive breast tumors, strikingly more (74.7% vs. 25.3%) specimens showed negative status of GREB1 protein, whereas in tumors with no or weak expression of EZH2, more (72.7% vs. 27.3%) samples exhibited positive staining of GREB1 (Fig. 6C). This suggests a significant inverse correlation between these two proteins ($P = 8.22E-08$; Fig. 6C). When we stratified the patient samples according to EZH2 or ERα protein levels, we found significantly more percentages of cases showing medium to strong staining of GREB1 when levels of EZH2 were low, whereas no to weak staining signals of GREB1 in samples with abundant EZH2 protein (Fig. 6D). Intriguingly, there was no such obvious correlation between ERα and GREB1 levels based on their IHC scores (Fig. 6D). All the data indicate that EZH2 and GREB1 are negatively correlated with each other in ER$^+$ breast cancer and that ERα may not be involved in EZH2-mediated repression of GREB1. Besides, in refractory breast tumors compared with the sensitive ones, EZH2 is dramatically upregulated ($P = 0.026$). Although not signifi-

cant ($P = 0.117$), GREB1 is markedly decreased. Again, ERα is equally expressed between responsive and resistant groups ($P = 0.68$; Fig. 6E). In summary, our results confirmed a strong negative correlation between EZH2 and GREB1 in clinical tumor samples, which may be firmly associated with cancer cell fate responding to tamoxifen.

Gene signature regulated by the ERα–EZH2–GREB1 axis represents a powerful predictive factor for the benefit of tamoxifen treatment in ER$^+$ breast cancer

We next stratified clinical follow-ups based on EZH2 and GREB1 levels (Fig. 7A). The tumors that were EZH2 positive and GREB1 negative had the worst clinical outcome of all (log-rank test $P = 7.8E-6$; Fig. 7A). We came to the same conclusion when we associated the clinical data with our IHC results (Fig. 7B). All these analyses indicate that combination of both EZH2 and GREB1 levels powerfully predicts breast cancer patients' responses to tamoxifen.

To further investigate the clinical significance of this gene-regulatory network consisting of EZH2, ERα, and GREB1, we defined gene signatures that were coregulated by EZH2 and ERα

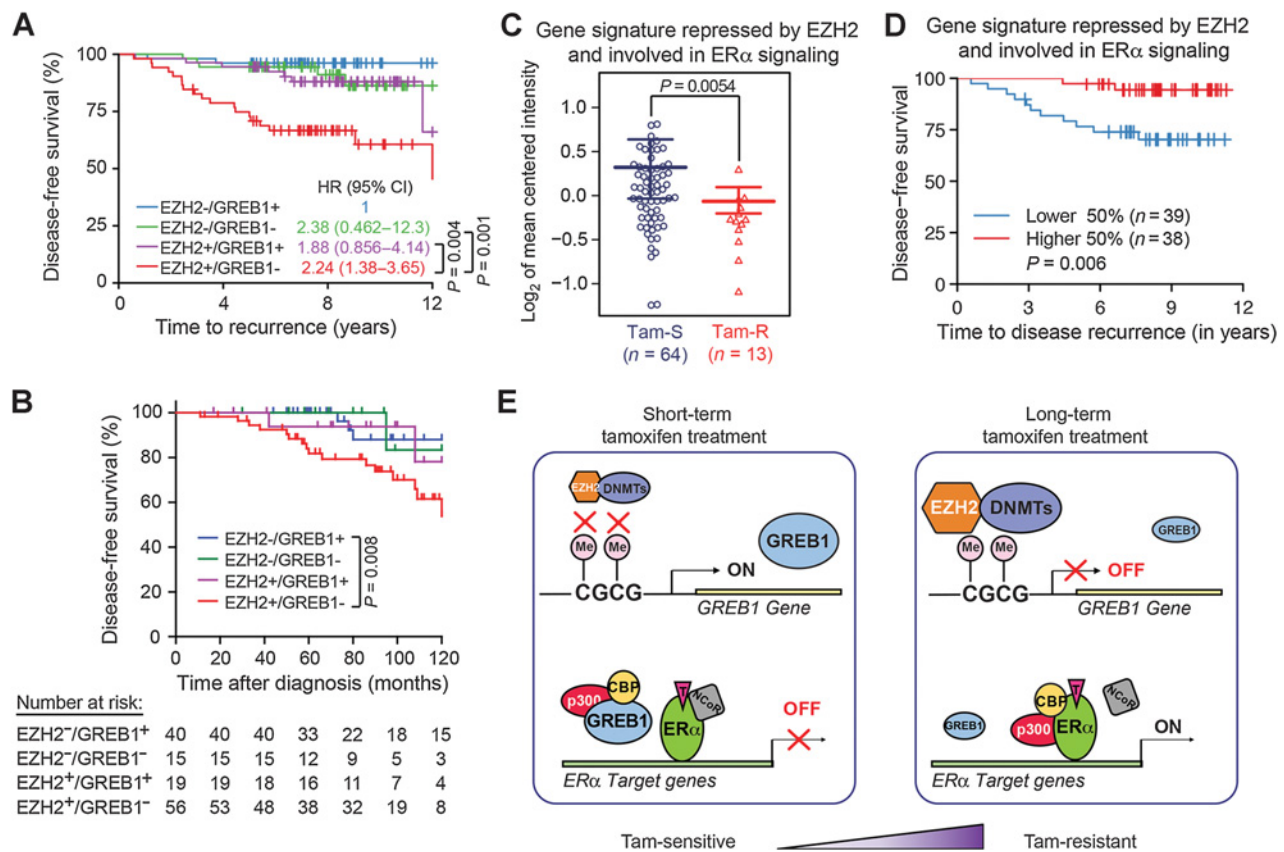**Figure 7.**
EZH2-mediated regulation of ERα signaling is highly clinical relevant to tamoxifen response. **A** and **B,** Kaplan–Meier curve showing disease-free survival rates in ER$^+$ breast tumors according to both EZH2 and GREB1 levels using GSE9195 and GSE12093 datasets (refs. 29, 30; **A**) and in 130 ER$^+$ breast cancer samples for IHC staining (**B**). +/−, expression level of top 50% (+) or bottom 50% (−) of the gene. **C** and **D,** Expression levels of gene signature that is repressed by EZH2 and involved in ERα signaling in tamoxifen-sensitive (Tam-S) or tamoxifen-resistant (Tam-R) breast tumors (**C**) and their prognostic power (**D**) using GSE9195 cohort (29). Figure legends represent the same meaning as in Fig. 1A and B. **E,** Model depicting the development tamoxifen resistance driven by the EZH2–ERα–GREB1 transcriptional axis. T, tamoxifen; Me, methylation.

signaling, and evaluated their therapeutic implications in two independent cohorts (29, 30). Interestingly, ERα target genes that are repressed by EZH2 were generally expressed at significantly lower levels in TamR breast cancer (Fig. 7C; Supplementary Fig. S8A), and their levels were positively associated with an improved disease-free survival (Fig. 7D; Supplementary Fig. S8B). However, genes that were dependent on ERα activity and simultaneously activated by EZH2 did not exhibit clear expression pattern or significant prognostic power in either dataset (Supplementary Fig. S8C–S8F). These results suggest that function of EZH2 as a transcriptional repressor dominates its biological role in conferring tamoxifen resistance in breast cancer cells. This also perfectly fits with our GSEA analysis of EZH2-regulated genes showing that functional annotations associated with endocrine resistance were only enriched in EZH2-repressed genes (Supplementary Fig. S2B). Therefore, targeting the ERα–GREB1–EZH2 axis holds promise for overcoming this major clinical challenge in the management of endocrine therapy–resistant ER$^+$ breast cancer.

Discussion

In ER$^+$ breast cancer, tamoxifen and other endocrine agents that suppress ERα signaling are highly effective in blocking tumor growth. However, loss of cellular sensitivity to endocrine therapy drastically limits the efficacy of the treatment, and substantial efforts have been put forth to search for new therapy options. In this study, we demonstrated that the epigenetic regulator EZH2 represents a promising target to overcome tamoxifen resistance, and indicated that impairing DNA hypermethylation at GREB1 promoter may be associated with the anticancer effects of EZH2-targeting drugs.

ERα cofactors demonstrate determinative roles in the regulation of ERα-mediated gene expression and further define the outcome of cellular responses to agonist or antagonist. Our study disclosed a key component in coordinating the regulatory proteins for proper ERα activity responding to different ligands, and that is GREB1. It has been demonstrated that GREB1 is required for binding of other coactivators with ERα upon estrogen stimulation (2). Here we showed that GREB1 was also essential for the formation of inactive ERα complex in response to tamoxifen. It blocked the association of key coactivators, such as p300 and CBP, with tamoxifen-liganded ERα, and subsequently the corepressor NCoR was recruited to the ERα-associated transcriptional complexes (Fig. 4B and C). This observation is pertinent to a previous discovery from the quantitative proteomic analysis that GREB1 interacts with estrogen-liganded, but not tamoxifen-liganded ERα (2). Therefore, GREB1 loses its binding capacity with ERα in the presence of tamoxifen and fails to bring essential coactivators for the formation of a functionally active complex. Validation of our model definitely needs further investigation. Particularly, biochemical evidence is required to demonstrate how other coactivators are restrained from ERα complex by GREB1 and why it is preferentially occur under antiestrogenic conditions. Understanding these questions will most likely provide promising therapeutic proteins or peptides for the effective treatment of endocrine-resistant breast cancer.

Multiple studies show that GREB1 is significantly downregulated in endocrine-resistant model systems, including cell lines and xenograft tumors (2, 35), and our work further confirmed in clinical samples (Fig. 6E). It is largely unknown how GREB1 gene is suppressed and what factors regulate its loss. Our data indicates that GREB1 is silenced by EZH2 and that DNA methylation may account for the epigenetic repression. Interestingly, we located a CpG-enriched site at GREB1 promoter, which is extensively methylated in endocrine resistant cell lines but devoid of the methylation signal in sensitive one (Fig. 3D). This striking difference in DNA methylation pattern is inversely correlated with the expression levels of GREB1 in clinical cases, highly suggesting that hypermethylation of this particular CpG site may account for the enduring downregulation of GREB1 in hormonal therapy–resistant breast cancer. More critically, methylation signals at some subsites within GREB1 promoter seem to positively associate with the pathologic stages of breast tumors, underscoring the potential clinical relevance of this specific epigenetic mark at this particular region. All the hypotheses definitely need further proof, especially in clinical scenarios.

As a histone methyltransferase, EZH2 orchestrates gene expression that determines cancer cell fate by directly methylating H3K27 at the promoters of downstream targets (9). Here we found that H3K27me3 was not remarkably detectable at GREB1 promoter (Supplementary Fig. S6A). Instead, EZH2 modulated DNA methylation levels at a specific CpG locus of the region and concurrent GREB1 expression (Fig. 3E–G; Supplementary Fig. S6H). However, we are still uncertain whether EZH2-mediated regulation of DNA methylation in our case is a direct in situ crosstalk, considering low levels of the repressive histone mark at the target promoter. We found that expression of DNMT1 and 3B was significantly decreased upon EZH2 silencing in TamR cells (Supplementary Fig. S6I). This result implies a positive control of methylation intensity at GREB1 promoter by EZH2, and meanwhile stimulates the interest to explore the relationship between EZH2 and DNA methylation in a genome-wide manner. Interestingly, global DNA hypermethylation has been repeatedly observed in endocrine-resistant cells, which led to decreased expression of central genes including key regulators of ERα activity (26, 36). These observations are in agreement with the findings from this study that EZH2 is overexpressed in refractory breast cancer and it positively regulates the levels and activities of DNMTs.

In summary, our work reveals a critical epigenetic program that determines ERα activity as well as cell fate in response to tamoxifen treatment (Fig. 7E). In sensitive cells upon short-term exposure of the antiestrogen, the presence of abundant GREB1 protein fails to recruit essential coactivators to ERα-binding sites and therefore induces a rapid inactivation of downstream target genes. However, long-term tamoxifen treatment results in altered activities of epigenetic enzymes such as EZH2 and DNMTs, which causes hypermethylation of GREB1 promoter. Maintenance of GREB1 protein at low levels reprograms ERα-dependent transcriptional machinery and induces a distinct transcriptome that renders refractory phenotypes in breast cancer cells. Taken together, our findings provide a compelling foundation for the clinical utility of selective EZH2 inhibitors for the treatment of ER$^+$, TamR breast cancer that expresses active epigenetic regulator EZH2 and harbors DNA hypermethylation at the specific CpG locus of GREB1 promoter region.

Disclosure of Potential Conflicts of Interest

Authors' Contributions

Acknowledgments

References

1. Ring A, Dowsett M. Mechanisms of tamoxifen resistance. Endocr Relat Cancer 2004;11:643–58.
2. Mohammed H, D'Santos C, Serandour AA, Ali HR, Brown GD, Atkins A, et al. Endogenous purification reveals GREB1 as a key estrogen receptor regulatory factor. Cell Rep 2013;3:342–9.
3. Rae JM, Johnson MD, Scheys JO, Cordero KE, Larios JM, Lippman ME. GREB 1 is a critical regulator of hormone dependent breast cancer growth. Breast Cancer Res Treat 2005;92:141–9.
4. Pathiraja TN, Nayak SR, Xi Y, Jiang S, Garee JP, Edwards DP, et al. Epigenetic reprogramming of HOXC10 in endocrine-resistant breast cancer. Sci Transl Med 2014;6:229ra41.
5. Elsheikh SE, Green AR, Rakha EA, Powe DG, Ahmed RA, Collins HM, et al. Global histone modifications in breast cancer correlate with tumor phenotypes, prognostic factors, and patient outcome. Cancer Res 2009;69: 3802–9.
6. Cardenas H, Zhao J, Vieth E, Nephew KP, Matei D. EZH2 inhibition promotes epithelial-to-mesenchymal transition in ovarian cancer cells. Oncotarget 2016;7:84453–67.
7. Ren G, Baritaki S, Marathe H, Feng J, Park S, Beach S, et al. Polycomb protein EZH2 regulates tumor invasion via the transcriptional repression of the metastasis suppressor RKIP in breast and prostate cancer. Cancer Res 2012;72:3091–104.
8. Lu C, Han HD, Mangala LS, Ali-Fehmi R, Newton CS, Ozbun L, et al. Regulation of tumor angiogenesis by EZH2. Cancer Cell 2010;18:185–97.
9. Cao R, Wang L, Wang H, Xia L, Erdjument-Bromage H, Tempst P, et al. Role of histone H3 lysine 27 methylation in Polycomb-group silencing. Science 2002;298:1039–43.
10. Vire E, Brenner C, Deplus R, Blanchon L, Fraga M, Didelot C, et al. The Polycomb group protein EZH2 directly controls DNA methylation. Nature 2006;439:871–4.
11. Kodach LL, Jacobs RJ, Heijmans J, van Noesel CJ, Langers AM, Verspaget HW, et al. The role of EZH2 and DNA methylation in the silencing of the tumor suppressor RUNX3 in colorectal cancer. Carcinogenesis 2010;31: 1567–75.
12. Rush M, Appanah R, Lee S, Lam LL, Goyal P, Lorincz MC. Targeting of EZH2 to a defined genomic site is sufficient for recruitment of Dnmt3a but not de novo DNA methylation. Epigenetics 2009;4:404–14.
13. McCabe MT, Ott HM, Ganji G, Korenchuk S, Thompson C, Van Aller GS, et al. EZH2 inhibition as a therapeutic strategy for lymphoma with EZH2-activating mutations. Nature 2012;492:108–12.
14. Knutson SK, Wigle TJ, Warholic NM, Sneeringer CJ, Allain CJ, Klaus CR, et al. A selective inhibitor of EZH2 blocks H3K27 methylation and kills mutant lymphoma cells. Nat Chem Biol 2012;8:890–6.
15. Xu K, Wu ZJ, Groner AC, He HH, Cai C, Lis RT, et al. EZH2 oncogenic activity in castration-resistant prostate cancer cells is Polycomb-independent. Science 2012;338:1465–9.
16. Feng Q, Zhang Z, Shea MJ, Creighton CJ, Coarfa C, Hilsenbeck SG, et al. An epigenomic approach to therapy for tamoxifen-resistant breast cancer. Cell Res 2014;24:809–19.
17. Morrison G, Fu X, Shea M, Nanda S, Giuliano M, Wang T, et al. Therapeutic potential of the dual EGFR/HER2 inhibitor AZD8931 in circumventing endocrine resistance. Breast Cancer Res Treat 2014;144: 263–72.
18. Liberzon A, Subramanian A, Pinchback R, Thorvaldsdottir H, Tamayo P, Mesirov JP. Molecular signatures database (MSigDB) 3.0. Bioinformatics 2011;27:1739–40.
19. Hurtado A, Holmes KA, Ross-Innes CS, Schmidt D, Carroll JS. FOXA1 is a key determinant of estrogen receptor function and endocrine response. Nat Genet 2011;43:27–33.
20. Zhang Y, Liu T, Meyer CA, Eeckhoute J, Johnson DS, Bernstein BE, et al. Model-based analysis of ChIP-Seq (MACS). Genome Biol 2008;9:R137.
21. Singletary SE, Allred C, Ashley P, Bassett LW, Berry D, Bland KI, et al. Revision of the American Joint Committee on Cancer staging system for breast cancer. J Clin Oncol 2002;20:3628–36.
22. Page DL, Ellis IO, Elston CW. Histologic grading of breast cancer. Let's do it. Am J Clin Pathol 1995;103:123–4.
23. Bachmann IM, Halvorsen OJ, Collett K, Stefansson IM, Straume O, Haukaas SA, et al. EZH2 expression is associated with high proliferation rate and aggressive tumor subgroups in cutaneous melanoma and cancers of the endometrium, prostate, and breast. J Clin Oncol 2006;24:268–73.
24. Harvey JM, Clark GM, Osborne CK, Allred DC. Estrogen receptor status by immunohistochemistry is superior to the ligand-binding assay for predicting response to adjuvant endocrine therapy in breast cancer. J Clin Oncol 1999;17:1474–81.
25. Lu R, Hu X, Zhou J, Sun J, Zhu AZ, Xu X, et al. COPS5 amplification and overexpression confers tamoxifen-resistance in ERalpha-positive breast cancer by degradation of NCoR. Nat Commun 2016;7:12044.
26. Stone A, Zotenko E, Locke WJ, Korbie D, Millar EK, Pidsley R, et al. DNA methylation of oestrogen-regulated enhancers defines endocrine sensitivity in breast cancer. Nat Commun 2015;6:7758.
27. Aryee MJ, Jaffe AE, Corrada-Bravo H, Ladd-Acosta C, Feinberg AP, Hansen KD, et al. Minfi: a flexible and comprehensive Bioconductor package for the analysis of Infinium DNA methylation microarrays. Bioinformatics 2014; 30:1363–9.
28. Cancer Genome Atlas Research Network. Comprehensive molecular portraits of human breast tumours. Nature 2012;490:61–70.

29. Loi S, Haibe-Kains B, Desmedt C, Wirapati P, Lallemand F, Tutt AM, et al. Predicting prognosis using molecular profiling in estrogen receptor-positive breast cancer treated with tamoxifen. BMC Genomics 2008;9:239.

30. Zhang Y, Sieuwerts AM, McGreevy M, Casey G, Cufer T, Paradiso A, et al. The 76-gene signature defines high-risk patients that benefit from adjuvant tamoxifen therapy. Breast Cancer Res Treat 2009;116:303–9.

31. Lavinsky RM, Jepsen K, Heinzel T, Torchia J, Mullen TM, Schiff R, et al. Diverse signaling pathways modulate nuclear receptor recruitment of N-CoR and SMRT complexes. Proc Natl Acad Sci U S A 1998;95:2920–5.

32. Wang L, Jin Q, Lee JE, Su IH, Ge K. Histone H3K27 methyltransferase Ezh2 represses Wnt genes to facilitate adipogenesis. Proc Natl Acad Sci U S A 2010;107:7317–22.

33. Knutson SK, Warholic NM, Wigle TJ, Klaus CR, Allain CJ, Raimondi A, et al. Durable tumor regression in genetically altered malignant rhabdoid tumors by inhibition of methyltransferase EZH2. Proc Natl Acad Sci U S A 2013;110:7922–7.

34. Hnatyszyn HJ, Liu M, Hilger A, Herbert L, Gomez-Fernandez CR, Jorda M, et al. Correlation of GREB1 mRNA with protein expression in breast cancer: validation of a novel GREB1 monoclonal antibody. Breast Cancer Res Treat 2010;122:371–80.

35. Cottu P, Bieche I, Assayag F, El Botty R, Chateau-Joubert S, Thuleau A, et al. Acquired resistance to endocrine treatments is associated with tumor-specific molecular changes in patient-derived luminal breast cancer xenografts. Clin Cancer Res 2014;20:4314–25.

36. Lin X, Li J, Yin G, Zhao Q, Elias D, Lykkesfeldt AE, et al. Integrative analyses of gene expression and DNA methylation profiles in breast cancer cell line models of tamoxifen-resistance indicate a potential role of cells with stem-like properties. Breast Cancer Res 2013;15:R119.

Cancer Research

AACR American Association for Cancer Research

Tamoxifen Resistance in Breast Cancer Is Regulated by the EZH2−ERα−GREB1 Transcriptional Axis

Yanming Wu, Zhao Zhang, Mauro E. Cenciarini, et al.

Updated version	Access the most recent version of this article at: doi:10.1158/0008-5472.CAN-17-1327
Supplementary Material	Access the most recent supplemental material at: http://cancerres.aacrjournals.org/content/suppl/2017/12/06/0008-5472.CAN-17-1327.DC1

Cited articles	This article cites 36 articles, 13 of which you can access for free at: http://cancerres.aacrjournals.org/content/78/3/671.full#ref-list-1

E-mail alerts	Sign up to receive free email-alerts related to this article or journal.
Reprints and Subscriptions	To order reprints of this article or to subscribe to the journal, contact the AACR Publications Department at pubs@aacr.org.
Permissions	To request permission to re-use all or part of this article, use this link http://cancerres.aacrjournals.org/content/78/3/671. Click on "Request Permissions" which will take you to the Copyright Clearance Center's (CCC) Rightslink site.